2012-01-1974

# Validation of a sparse analytical Jacobian chemistry solver for heavy-duty diesel engine simulations with comprehensive reaction mechanisms

**Federico Perini[1,2], G. Cantore[1], E. Galligani[1], R.D. Reitz[2]**
[1]University of Modena and Reggio Emilia
[2]University of Wisconsin-Madison

## ABSTRACT

The paper presents the development of a novel approach to the solution of detailed chemistry in internal combustion engine simulations, which relies on the analytical computation of the ordinary differential equations (ODE) system Jacobian matrix in sparse form. Arbitrary reaction behaviors in either Arrhenius, third-body or fall-off formulations can be considered, and thermodynamic gas-phase mixture properties are evaluated according to the well-established 7-coefficient JANAF polynomial form. The current work presents a full validation of the new chemistry solver when coupled to the KIVA-4 code, through modeling of a single cylinder Caterpillar 3401 heavy-duty engine, running in two-stage combustion mode. The code has been tested on a wide range of simulations, at different injection timings, intake pressures, and EGR mass fractions, and considering two reaction mechanisms: a skeletal one with 29 species and 52 reactions, and a comprehensive, semi-detailed one with 160 species and 1540 reactions. The results show that the developed approach allows computational time savings of more than one order of magnitude in comparison to a reference chemistry solver, even with no reduction of the combustion mechanism size.

## INTRODUCTION

The increasing demand for fuel efficiency and environmental sustainability of internal combustion engines is driving research towards the exploration of new combustion concepts, which heavily rely on the interactions between fuel chemistry and mass transport within the combustion chamber [1, 2]. In addition, the need to achieve reliable predictions of local properties, such as species concentrations and temperatures, and their evolution during the combustion process, has led to the progressive introduction of chemical kinetics codes coupled with computational fluid dynamics (CFD) solvers [3, 4]. Quantitative chemistry modeling capabilities have thus been achieved by adopting tailored reaction mechanisms, whose impact on the CFD solver is usually part of an operator splitting procedure, and yields source terms for species mass fractions and cell internal energy due to the combustion chemistry. The main ignition characteristics have been shown to be correctly captured even with skeletal reaction mechanisms, made up of few species and few dozen reactions, and thus have enabled the study of homogeneous combustion modes such as the HCCI [1]. However, newer combustion concepts require that more comprehensive models are introduced, as they exploit different reactive regions of the air-fuel mixture, or multiple fuels acting within the combustion chamber [2], or fuels whose complex composition needs to be modeled as a blend of different compounds [5, 6].

The reaction mechanism literature is indeed trending to a dramatic increase in the overall mechanism dimensions for common fuels, due to the need to consider the whole chain of species classes, ranging from the smallest species to the longest molecular structures [7]. As a matter of fact, some of the most recently presented detailed mechanisms feature up to about 3,000 species and 10,000 reactions [8]; and their adoption for studying combustion systems of industrial interest is practically unviable. The computational complexity of the integration of the system of ordinary differential equations (ODE) for the reaction mechanism, which has to be solved in each cell of the multidimensional CFD domain, scales with $n_s^3$, $n_s$ being the number of species considered in the reaction mechanism, due to factorization of the Jacobian matrix [7]. The chemistry ODE system is also usually characterized by severe stiffness, with very fast reactions coexisting with very slow reaction sets. Thus, explicit integration methods which do not require Jacobian matrix evaluation appear to be unsuitable due to unacceptably small integration steps.

In this framework, a number of techniques have been developed with the aim of reducing the complexity of the solution of the ODE system associated to the reaction mechanism. Most of them aim at reducing the mechanism's size or stiffness, while keeping the error

introduced by the simplification under control (see, for example, [9-11]). In this work, the application of a newly developed approach for the solution of combustion chemistry ODE systems in CFD codes [12] is presented. Our approach aims at reducing the computational requirements due to the integration of the chemistry ODE system by adopting an exact, sparse analytical Jacobian formulation for the constant volume initial value problem (IVP), without changing the reaction mechanism features. Reduced computational demand can enable semi-detailed, comprehensive mechanisms made up of hundreds species and about one thousand reactions to be used for multidimensional CFD simulations with detailed chemistry. The adoption of a similar approach, in comparison to more common and widely used methodologies for on-the-fly mechanism reduction or stiffness removal, appears to be competitive for internal combustion engine simulations for the following reasons:

- Sparsity of the matrix algebra associated to the mechanism is significant even on skeletal mechanisms with tens of reactions and species, as often only elementary reactions are included, and anyway usually not more than three reactants and products per reaction are present;
- Computational demand for the evaluation of the Jacobian matrix scales with $n_s^2$ when using finite-difference approximation, as done as default by ODE solvers, while it can be significantly reduced when evaluating only the non-zero elements analytically, and in sparse form;
- Internal Newton's iteration convergence is improved up to quadratic in the case where the exact Jacobian matrix is evaluated;
- The approach considers the integration of the entire reaction mechanism, thus avoiding the introduction of sources of error.

An analytical Jacobian formulation for arbitrary initial value problems of chemical kinetics in adiabatic constant volume environments has thus been developed and proposed, considering gas-phase thermodynamics in the JANAF 7-coefficient polynomial form [13]. The code includes three possible reaction behaviors, including simple Arrhenius-type reactions, third-body reactions with effective molecularity coefficients, and fall-off reactions in Lindemann's and Troe's forms [12, 14]; these formulations usually cover most reaction mechanisms of interest to the combustion community. The validation of the proposed methodology has been assessed by comparison to the reference chemical kinetics package CHEMKIN-II [15], and shows excellent agreement in terms of predicted quantities. Good computational time savings that range from about 50% time for a skeletal combustion mechanism for n-heptane, up to more than one order of magnitude for a detailed reaction mechanism for primary reference fuels (PRF) have been observed. The chemical kinetics code developed has then been implemented into a custom version of the KIVA-4 program, and used to model a heavy-duty single cylinder test engine, the Caterpillar SCOTE 3401E, operating with two-stage combustion, and running under a variety of conditions that feature different injection pulse timings as well as boost pressures. The validation shows that simulations of the closed-valve part of the engine cycle, using a comprehensive reaction mechanism for n-heptane made up of 160 species and 1540 reactions, and with a refined sector mesh with more than 40,000 cells at bottom dead center (BDC) can be completed in less than 100 hours on a 4-CPU machine.

This paper is structured as follows: in the following paragraph the most important details of the sparse analytical Jacobian approach are presented, and discussed by comparing four reaction mechanisms widely used in the combustion community; then, validation of the approach for constant-volume reactor simulations is provided by comparing the results obtained from the CHEMKIN-II package; finally, modeling and validation results of the Caterpillar SCOTE engine are presented, considering two different computational grids and two different reaction mechanisms for n-heptane combustion.

# THE SPARSE ANALYTICAL JACOBIAN APPROACH

The most important equations driving the sparse analytical Jacobian approach for combustion chemistry are described here. The implementation has been made within a framework, in Fortran, previously developed [14, 16] for thermodynamic properties and reaction kinetics of gas-phase species. A full derivation of the Jacobian elements, also including the derivatives of the thermodynamic functions and potentials involved is described in detail in [12].

## CONSTANT VOLUME INITIAL VALUE PROBLEM

The integration of chemical kinetics within the operator-splitting procedure adopted by most multidimensional CFD solvers computes the species and internal energy source terms of each cell in the domain as those arising within adiabatic constant-volume environments, where a number of reactions occur. In particular, a set of $n_r$ reactions, involving a total number of species $n_s$, is expressed as:

$$\sum_{i=1}^{n_s} \nu'_{k,i} M_i \rightleftharpoons \sum_{i=1}^{n_s} \nu''_{k,i} M_i , \quad k = 1, \dots, n_r, \tag{1}$$

where the stoichiometric coefficients of reactants $\nu'_{k,i}$ and products $\nu''_{k,i}$ are stored in sparse matrices, and $M_i$ identify the chemical labels of the species involved in the mechanism. Since the stoichiometric coefficients for each of the reactions in the mechanism

verify conservation of elements, the global mass conservation within the system can be expressed as a system of $n_s$ differential equations involving the species mass fractions $Y_i$. The contributions of each reaction to each species rate of change are accounted for as:

$$\frac{dY_i}{dt} = \frac{W_i}{\rho}\sum_{k=1}^{n_r}\left(\nu''_{k,i} - \nu'_{k,i}\right) q_k, \tag{2}$$

with $W_i$ the molecular weight of the $i$-th species, and $\rho$ the average constant mixture density. The rate of progress variable for the $k$-th reaction, $q_k$, is dependent on the reaction behavior, thus usually on the system temperature $T$, and on the mass fractions $Y_j$ of the species which are directly or indirectly involved in the reaction. For the simplest behavior, typical of elementary reactions, the rate of change of progress variable follows the law of mass action in the forward and backward reaction directions:

$$q_k = q_{f,k} - q_{b,k} = k_{f,k}\prod_{i=1}^{n_s}\left(\frac{\rho Y_i}{W_i}\right)^{\nu'_{k,i}} - k_{b,k}\prod_{i=1}^{n_s}\left(\frac{\rho Y_i}{W_i}\right)^{\nu''_{k,i}}. \tag{3}$$

In this case, the forward reaction rate constant has an Arrhenius expression:

$$k_{f,k} = A_k\, T^{b_k}\, exp\left(-\frac{E_k}{R_u\, T}\right), \tag{4}$$

and the backward reaction rate constant $k_{b,k}$ can either be defined by a similar Arrhenius expression, or computed from knowledge of the equilibrium constant of the reaction: $K_{eq,k} = k_{f,k}/k_{b,k}$.

Third-body reactions describe how the presence of other species in the gaseous mixture than the ones participating in the reaction itself increases and modifies the probability of active collisions between them. In these reactions, the more complex dependence on the species is considered through an effective molecularity, $M_{eff,k}$, that multiplies the standard rate of progress variable of Equation (3), and contains the sum of each species' molar concentration, multiplied by a weighting factor, the effective molecularity coefficient:

$$M_{eff,k} = \sum_{i=1}^{n_s}\left(\alpha_{k,i}\frac{\rho Y_i}{W_i}\right) = C_{tot} - \sum_{i=1}^{n_s}\left(\beta_{k,i}\frac{\rho Y_i}{W_i}\right); \tag{5}$$

$$q_{TB,k} = M_{eff,k}\, q_k. \tag{6}$$

The effective molecularity of the species can be expressed as a real coefficient $\alpha_{k,i}$, that is generally equal to one for most species or $\beta_{k,i} = 1 - \alpha_{k,i}$ , as for example shown in [17]. $\beta_{k,i}$ is non-zero only for the species whose molecular geometry leads to an enhanced impact onto the reaction. $C_{tot}$ expresses the total average mixture concentration in molar units (e.g., $mol/cm^3$ in CGS units).

The effective molecularity value of Equation (5) is also present in pressure-dependent reactions, where the dilute gas hypothesis that is the basis of the Arrhenius formulation is not suitable to describe the reaction behavior at different pressures. In this case, two Arrhenius formulations are needed to describe the reaction at the low- and high-pressure limits (through two different forward reaction rate constants, $k_{f,k,\infty}$ and $k_{f,k,0}$). The resulting effective reaction rate constant at pressure $p$ is given by:

$$k_{PD,f,k} = k_{f,k,\infty}\, F_k^{PD}, \tag{7}$$

where $F_k^{PD} = F_k^{PD}\left(p, M_{eff,k}, k_{f,k,\infty}, k_{f,k,0}\right)$ is a function that balances the two extreme values at the pressure limits. Two of the most widely adopted formulations for $F_k^{PD}$, according to Lindemann and Troe have been considered in the present approach [18]:

$$q_{PD,k} = F_k^{PD}\, q_k. \tag{8}$$

Overall, the reaction rate formulations contribute to evaluating the instantaneous rates of change of mass fractions in the system from Equation (2). In the constant-volume reactor, one more differential equation for energy conservation closes the problem. It expresses the change in the system's internal energy due to the modified mixture composition:

$$\frac{dT}{dt} = -\frac{1}{\bar{c}_v}\sum_{i=1}^{n_s}\left(\frac{U_i(T)}{W_i}\frac{dY_i}{dt}\right), \tag{9}$$

where $\bar{c}_v$ represents the average mixture specific heat at constant volume in mass units, and $U_i$ the internal energy of the species in molar units.

Equations (2) and (9) thus build up the complete constant-volume reactor initial value problem, where the unknowns are represented by a $(n_s + 1 \times 1)$ column array, $\boldsymbol{y} = [T \quad Y_1 \quad \cdots \quad Y_{n_s}]^T$:

$$\boldsymbol{y}' = \boldsymbol{f}(\boldsymbol{y}) = \begin{bmatrix} dT/dt \\ dY_1/dt \\ \cdots \\ dY_{n_s}/dt \end{bmatrix}, \boldsymbol{y}(0) = \boldsymbol{y_0}. \tag{10}$$

# JACOBIAN MATRIX STRUCTURE

The Jacobian matrix of the constant-volume IVP represented by Equation (10) contains the derivatives of the rates of change for temperature and species mass fractions with respect to the unknowns,

$$J_{i,j} = \frac{\partial f_i}{\partial y_j}, \qquad i,j = 1, \dots, n_s + 1, \tag{11}$$

and has a sparse bordered structure, as represented in Figure 1. The first column and the first row are dense, and contain the derivatives of the ODE system vector function with respect to temperature, and the derivatives of temperature rate of change with respect to the species mass fractions, respectively. The inner matrix block is instead sparse, and contains the derivatives of the species mass fraction rates of change with respect to the species mass fractions themselves. As far as the sparsity of this block is concerned, an important role is played by species involved in third-body, or in pressure-dependent reactions, that have nonzero derivatives with respect to any other species mass fraction. In fact, the derivatives of the effective molecularity formulation of Equation (5) with respect to each species is nonzero in constant volume environments. This leads to full dense lines in the Jacobian matrix corresponding to each species involved in third-body reactions. However, a simplifying assumption has been made, that in constant volume environments not only is the overall mass density constant, but also the overall concentration in mole units $C_{tot}$ does not change significantly. Then the derivatives of the effective molecularities with respect to the species that have $\beta_{k,i} = 0$ in Equation (5) can be neglected, thus resulting in much more sparse rows. This assumption was first proposed by Schwer et al. [17], and applied to constant-pressure environments, where the overall concentration in mole units is constant by definition. It has however been verified that this assumption for building the Jacobian matrix is perfectly suitable for constant-volume environments too [12], and that it does not lead to noticeable differences during the numerical integration. Moreover, it significantly increases the Jacobian matrix sparsity.

$$\mathbf{J} = \begin{array}{|c|c|} \hline \dfrac{\partial \dot{T}}{\partial T} & \dfrac{\partial \dot{T}}{\partial Y_j} \\ \hline \dfrac{\partial \dot{Y}_i}{\partial T} & \dfrac{\partial \dot{Y}_i}{\partial Y_j} \\ \hline \end{array}$$

***Figure 1 – Jacobian matrix structure for the constant-volume reactor.***

The full derivation of the Jacobian matrix in sparse form is beyond the scope of this paper, but it has been completely reported in [12].

The sparsity of the Jacobian matrix is strongly influenced by the reaction mechanism's dimensions, as shown in Figure 2. Here, the matrix sparsity patterns of three reaction mechanisms widely used for modeling and simulating diesel combustion are represented: the first mechanism, by Patel et al. [19] ("ERC mechanism"), is a skeletal model for n-heptane combustion, made up of 29 species and 52 reactions, that has been extensively adopted for HCCI and PCCI diesel engine simulations. The second one, by Seiser et al. [20], has 160 species and 1540 reactions, and is a semi-detailed mechanism for n-heptane oxidation. The last, by Curran et al. [21], is the most complete one, models the oxidation of primary reference fuels (PRF) mixtures, and contains 1034 species and 4236 reactions. These mechanisms' sparsity features are summed up for reference in Table 1, where also the details of the methyl-decanoate oxidation mechanism by Herbinet et al. [22] are included, as they represent typical current maximum mechanism dimensions. From the images in Figure 2, it is interesting to notice that even the smallest mechanism has a significant Jacobian sparsity value, greater than 50%. The number of blank elements increases dramatically with the reaction mechanism size, and reaches values around or greater than about 90% for the large mechanisms.

***Table 1 – Jacobian matrix sparsity features for the constant volume initial value problem for the four reaction mechanisms considered, according to the sparse third-body formulation.***

| **Mechanism** | **$n_s$** | **$n_r$** | **non-zero** | **sparsity** |
|---|---|---|---|---|
| 1. ERC n-heptane | 29 | 52 | 412 | 54.2% |
| 2. LLNL n-heptane | 160 | 1540 | 3570 | 86.2% |
| 3. LLNL PRF | 1034 | 4236 | 22551 | 97.9% |
| 4. LLNL MD | 2878 | 8555 | 166703 | 99.4% |

The increase in Jacobian matrix sparsity with increasing mechanism dimension is mainly caused by the limited number of species that usually participate in each reaction. Also the number of species owning enhanced molecularity coefficients in third-body and pressure dependent reactions – i.e., $\beta_{k,i} \neq 0$ – is typically limited to not more than 5-10 important species in typical reaction mechanisms. As a consequence, the computational requirements due to evaluation of the Jacobian matrix are strongly influenced by its sparsity, as shown in Figure 3. Here, the CPU times needed by the Fortran code developed to evaluate (1) the constant-volume ODE system function, (2) the exact sparse Jacobian matrix using sparse matrix algebra, and (3) the approximated Jacobian matrix using finite differences for the four reaction mechanisms of Table 1 are plotted. The plot shows that a very strong reduction in CPU times can be achieved through the evaluation of the Jacobian in analytical and sparse form. This reduction is of about four times less than the finite-difference estimation even for the smallest mechanism, and increases to more than 40 times for the methyl-decanoate mechanism. The effects of the computational time savings still remain significant when considering the total CPU time taken for the integration of 18 constant-volume reactor problems, whose conditions are described in the following paragraph. The same program, with the same ODE solver setup, but evaluating the Jacobian matrix in sparse analytical form is capable of completing the integration in a total time about one order of magnitude less than the same program with the standard finite-difference Jacobian approach.

# VALIDATION OF THE CHEMISTRY SOLVER

The CPU time requirements analyzed in the previous section have highlighted the strong computational performance of the sparse Jacobian matrix approach that allowed significant time savings in comparison with the traditional finite-difference strategy adopted by most ODE integrators when dealing with complex problems. In order to validate the numerical accuracy of the developed code, a first comparison with the CHEMKIN-II package was made for zero-dimensional, adiabatic constant-volume reactors, and only as a second step was the code integrated into the KIVA-4 code for multidimensional modeling of a heavy-duty engine.

## CONSTANT VOLUME REACTORS

In order to test each of the reference mechanisms at a variety of reactive conditions, a simulation landscape similar to that adopted in [16, 23] was used. In particular, a matrix of 18 IVP integration cases was considered, corresponding to the possible combinations of two initial pressure values, $p_0 \in \{2.0; 20.0\}\ bar$, three initial air-fuel mixture equivalence ratios, $\phi_0 \in \{0.5; 1.0; 2.0\}$, and three initial reactor temperatures: $T_0 \in \{750; 1000; 1500\}\ K$. The definition of such a landscape was chosen in order to include, as much as possible, low- and high-temperature chemistry, low- and high-pressure cases, plus different mixture conditions typical to those occurring in compression ignition engines. From the ODE system integrator point of view, these cases also corresponding to a variety

of stiffness conditions that represent perhaps the most important factor affecting the ODE solver's performance. For the sake of completeness, the total integration time for each case was chosen by evaluating its predicted mixture ignition delay time, and using approximately 1.5 times the ignition event. Then, each integration interval was subdivided in 100 equally-spaced integration sub-steps. This last choice was motivated by the fact that most implicit ODE solvers (such as VODE [24] and LSODE [25, 26], as described next) are capable of reaching wide integration steps, and often jump after transient conditions. By subdividing the integration interval we instead tried to reproduce the integration conditions occurring when the ODE solver is coupled to a CFD code, and the detailed chemistry source terms need to be evaluated as a part of an operator-splitting procedure where the overall advancement time-step is ruled by the multidimensional code.

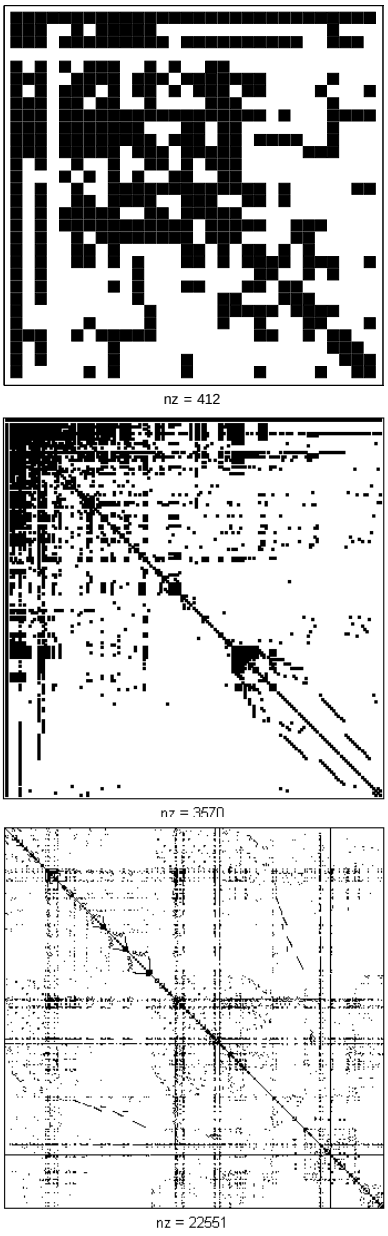


***Figure 2 – Jacobian matrix sparsity patterns for the constant volume problem: (top) ERC n-heptane mechanism, (center) LLNL reduced n-heptane mechanism, (bottom) LLNL PRF mechanism.***

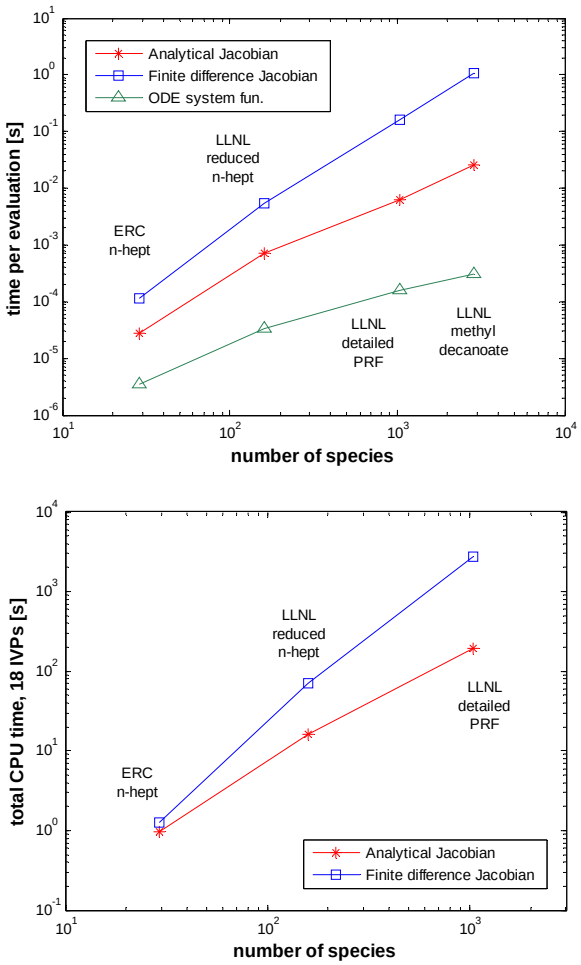


***Figure 3 – (top) CPU time requirements for the evaluation of chemistry ODE system function and Jacobian matrix, in both analytical exact and finite-difference approximated forms. (bottom) cumulative CPU times over 18 integration problems, finite-difference Jacobian vs. sparse analytical formulation.***

Figure 4 shows the validation, in terms of the predicted mass fraction profiles of some important species, with the sparse analytical Jacobian chemistry code and the CHEMKIN-II package CONV application, integrated using the VODE solver. The plots represent the time evolution of the species in the case with initial pressure $p_0$ = 2.0 bar, initial reactor temperature $T_0$ = 750 K, and initial equivalence ratio $\Phi_0$ = 1.0. The integration has been performed using the LSODES solver, at the same integration tolerances as used for the CHEMKIN package: RTOL = $10^{-4}$, ATOL = $10^{-13}$. Even if the LSODES does not use variable-coefficient methods (acknowledged to make VODE often computationally much more efficient [27]) it was chosen for the integration with the sparse code as it includes sparse algebra routines for the Jacobian matrices provided in sparse form. The ODE solver integration settings are also summarized in Table 2.

***Table 2 – Summary of the solver settings for the two compared chemistry codes.***

| Program | CHEMKIN-II | present code |
|---|---|---|
| ODE solver | VODE [24] | LSODES [25] |
| relative tolerance | $10^{-4}$ | $10^{-4}$ |
| absolute tolerance | $10^{-13}$ | $10^{-13}$ |

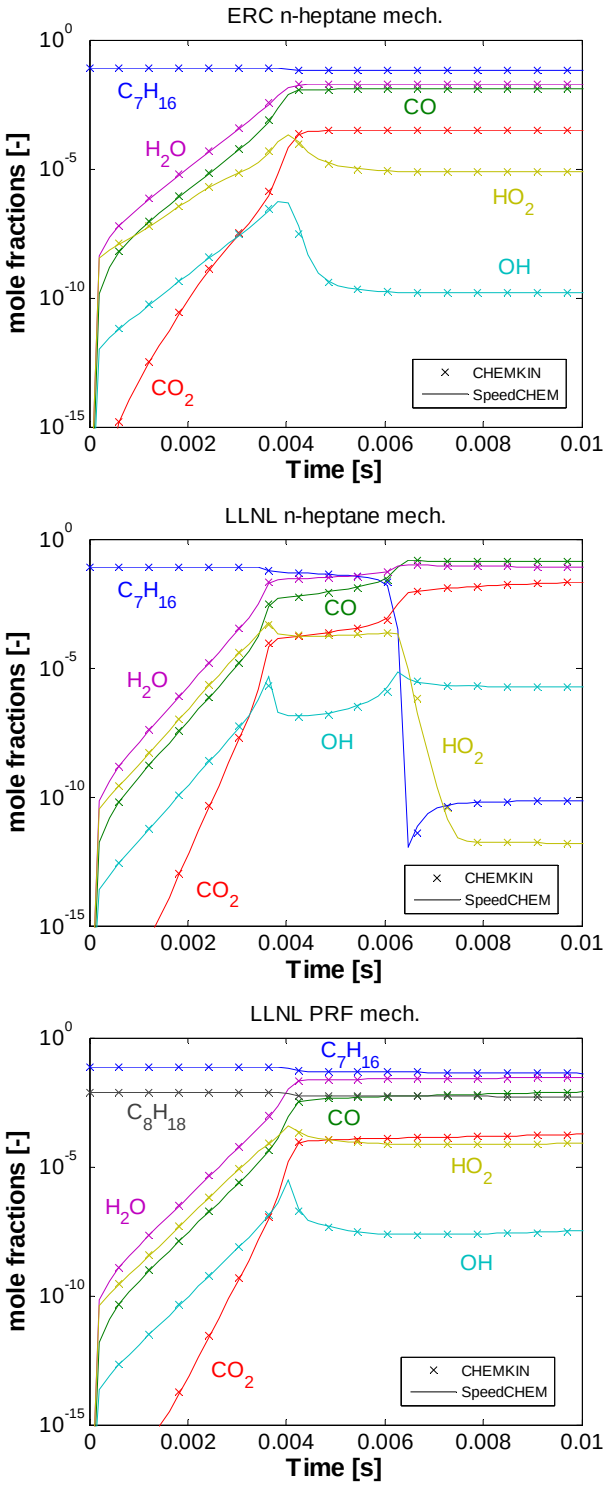


***Figure 4 – Predicted mass fraction profiles for IVP validation: $p_0$ = 2 bar, $T_0$ = 750 K, $\Phi_0$ = 1.0. Mechanisms: ERC n-heptane (top), LLNL n-heptane (top), LLNL PRF (bottom), with fuel mass fractions: 90% n-heptane, 10% iso-octane. Chemkin-II (marks) vs. present code (lines).***

From the results, no significant differences can be observed when looking at the predicted species mass fraction profiles using the two codes, even at the smallest values (i.e., $<10^{-15}$). Thus, it appears that the computational accuracy of the solver is robust, and the results always follow the solution predicted by CHEMKIN. The most important achievement is the reduced overall CPU times needed by the integration. In Figure 5 the cumulative amount of time needed by the integration of the 100 partial steps for all 18 IVPs is plotted. The figure shows that a significant CPU time speedup of about 1.89 times is achieved even at the skeletal mechanism, where the integration took about 0.95 seconds on an Intel i7 920 machine, while the CHEMKIN integration required on the same machine about 1.80 seconds. The speedup is maximum and is around 32.6 times when using the large PRF mechanism. Only 193.1 seconds were needed for the integration when adopting the present code while the CHEMKIN calculation was completed in about 6302.5 seconds. The figure also shows an almost linear increase in the overall speedup factor, which is clearly mechanism-dependent, but that suggests that the best computational achievements can be reached for the largest mechanisms, thus making the code implemented with the analytical Jacobian approach particularly suitable for incorporating full large-scale mechanisms into multidimensional simulations.

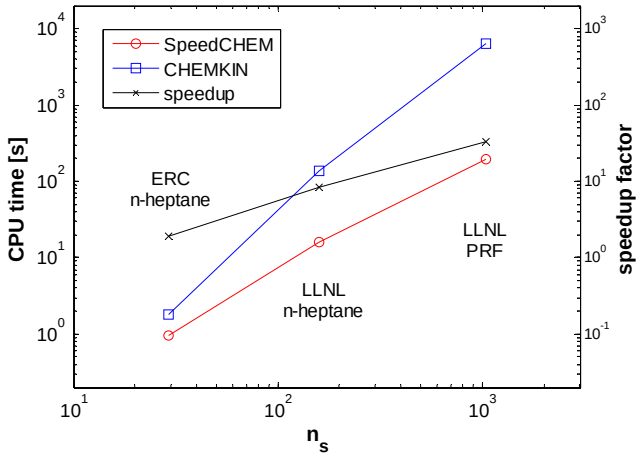


***Figure 5 – CPU times for the integration of the 18 IVP cases considered. CHEMKIN-II (blue) vs. analytical Jacobian chemistry code (red) comparison. Speedup factors in black cross marks.***

## MODELLING OF A HEAVY-DUTY DIESEL ENGINE

As the aim of the proposed approach is to achieve enough computational efficiency to incorporate detailed reaction kinetics when modeling practical combustion systems, the present code was coupled with a custom version of the KIVA-4 [28] CFD code. Here, detailed chemistry is accounted for through species and internal energy source terms that are introduced in each cell of the engine grid, and at each advancement time step, provided that the internal cell temperature is greater than a user-specified value, e.g., 500 K. Caterpillar Single-Cylinder Oil Test Engine (SCOTE) 3401 experiments were carried out by Hardy [29], and have been used as a reference for the validation of engine CFD models (see, for example, [30, 31]). The detailed engine specifications, including the experimental apparatus, can be found in [29], and a brief summary of the main engine details is also reported in Table 3.

The engine was operated in a two-stage combustion mode, featuring double injections: a pilot injection pulse injected about 50-60 degrees before top dead center, and the main injection around TDC. The validation was made for the baseline operating condition, with pilot injection starting at -56.5 °ATDC and lasting for 1450 μs, and the main injection pulse starting 5 degrees before TDC and lasting for 1950 μs. Further comparisons between the computational models and the experimental measurements were made at varying main injection timings, pilot injection timings, and intake boost pressures. A summary of the operating conditions is reported in Table 4.

***Table 3 – Caterpillar SCOTE 3401 engine details [29].***

| | |
|---|---|
| Engine type | direct-injection diesel |
| Number of cylinders | 1 |
| Valves per cylinder | 4 |
| Bore x Stroke [mm] | 137.2 x 165.1 |
| Conrod length [mm] | 261.6 |
| Compression ratio [-] | 16:1 |
| Unit displacement [L] | 2.44 |
| Chamber Turbulence | Quiescent |
| Piston bowl geometry | Mexican hat |

***Table 4 – Engine operating conditions.***

| | |
|---|---|
| Rotating speed [rev/min] | 1737 |
| Engine load [-] | 57% |
| Intake temperature [K] | 305.15 |
| Injection rate [g/s] | 1.94 |
| Pilot injection start [°atdc] | -65 ÷ -50 |
| Pilot injection length [μs] | 1000 ÷ 1450 |
| Main injection start [°atdc] | -5 ÷ 20 |
| Main injection length [μs] | 1950 |
| EGR fraction | 0 % |
| Boost pressure [kPa] | 186.2 ÷ 220.6 |

## MODEL DETAILS

Modeling of the Caterpillar engine was conducted using a custom version of the KIVA-4 code [14]. The code has been provided with detailed chemistry capability, and all the species existing in the reaction mechanism are shared with the fluid flow solver. Also the CHEMKIN-II CONV program [15], for constant volume computations, integrated with the VODE solver [24], was coupled to KIVA for providing a reference solution to be compared with the developed chemistry solver. As far as the liquid fuel spray is concerned, the thermo-physical properties of $C_{14}H_{30}$ were chosen for the computation, and the standard KIVA-4 spray dynamics, breakup and evaporation models were used. Coalescence between liquid droplets was deactivated due to its known grid-dependent behavior [32]. Finally, a dynamic injection spray angle model has been implemented, following the formulation by Reitz and Bracco [33], as already applied and tested in [34] for high pressure diesel fuel sprays.

Detailed combustion chemistry was simulated considering the first two mechanisms for n-heptane oxidation listed in Table 1. Added to both of them were twelve reactions for nitrogen oxides formation extracted from the GRI-mech [35], as suggested by Cantrell et al. [30]. The overall mechanism dimensions were hence 34 species and 64 reactions for the ERC+NOx mechanism, and 165 species and 1552 reactions for the LLNL n-heptane+NOx mechanism.

Two different engine grids were prepared for the engine model using the K3PREP pre-processor. The first, “coarse” one, contains 16950 cells at bottom dead center, and represents typical sector mesh dimensions that can be adopted with robust spray models, that exhibit limited grid dependency. A second, “refined” mesh was made of 42480 cells at BDC, and has a spatial resolution of about 1.1 mm. Both grids are 60-degree cylinder sectors with periodic boundary conditions at the sector interfaces. A smooth cell layer snapping algorithm has been used for allowing at least four cell layers to be present when the piston reaches TDC so as to correctly model thermal and turbulent boundary layers. The grids were also refined at the cylinder walls for the same reason. In Figure 6 the two grids are shown at top dead center.

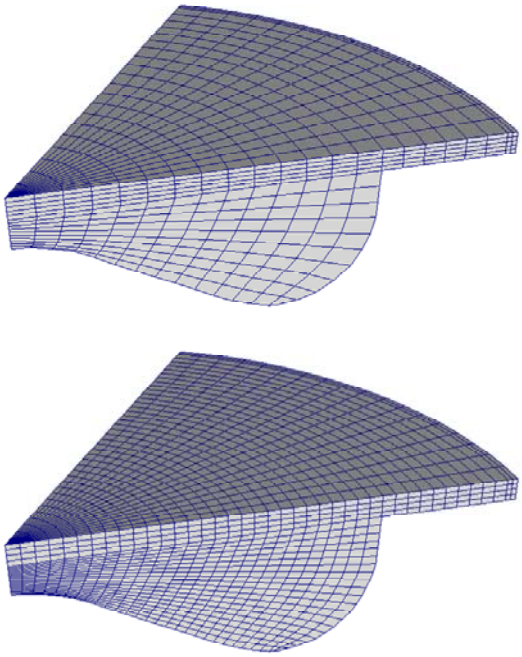

***Figure 6 – Coarse (top) and refined (bottom) grids for the Caterpillar SCOTE engine, at top dead center.***

## RESULTS

First, the model validation was carried out at the reference operating condition, with particular focus on comparing the computational accuracy and performance of the model when using both grids, and when adopting the two reaction mechanisms. In Figure 7 the predicted average in-cylinder pressure and apparent heat release are reported. The comparisons between solutions using the two different chemistry solvers for both grids show an excellent agreement. This confirms the robustness of the sparse analytical Jacobian code. The most significant differences occur between the two grids, in particular, for the prediction of the main ignition event after the cool flame region. According to the refined mesh calculation, it occurs in the squish region, as it can be noticed from Figure 8, where the oxygen concentrations are plotted during the main ignition event. This same behavior is also observed when adopting the large LLNL reaction mechanism, where a similar predicted ignition timing of the premixed mixture from the pilot injection is seen about 1.5 crank angle degrees later.

Figure 9 summarizes the overall CPU time demands of the simulations. In particular, the bar graph shows that even on the small mechanism scale the analytical Jacobian chemistry solver is able to reduce by about 2 times the overall CPU time for the KIVA simulation, also considering the fixed CPU time amount used by the flow field solver part of the code. The CPU time requirements that are reported when using the LLNL mechanism represent a semi-parallel solution, where the chemistry solver load has been subdivided in parallel on 4 CPUs, adopting the OpenMP shared memory parallel paradigm [36] to subdivide the cell domain. The coarse grid simulation ran in 24.59 hours, thus being suitable for simulations of practical industrial interest, and also the refined grid time scaled almost linearly with the number of cells, requiring a total of 89.55 hours to be completed. On the average, the computational time saving when adopting the present chemistry solver on both grids was about 75.4%.

In order to complete the present validation, analyses in terms of pollutant emissions (nitrogen oxides) were made for varying start of injection for the pilot and the main injection pulses, and the cylinder boost pressures, and the results are reported in Figure 10.

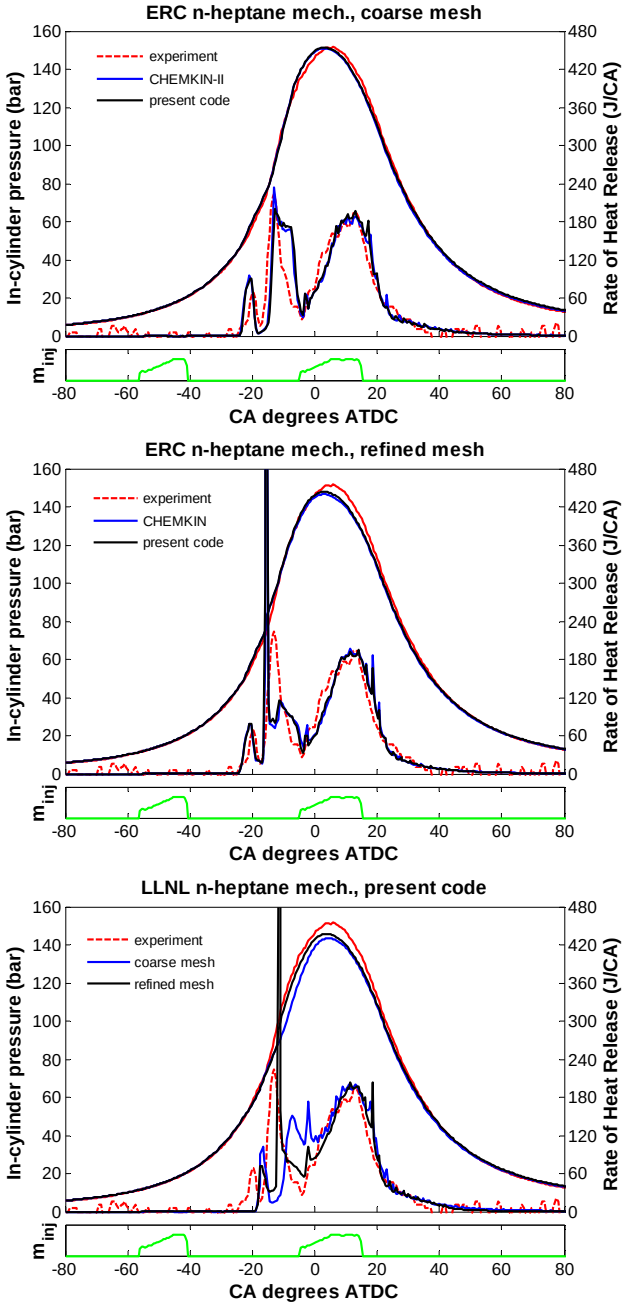


***Figure 7 – Predicted in-cylinder pressure and apparent heat release validation case with both n-heptane mechanisms: ERC mechanism at coarse (top) and refined (center) mesh Chemkin-II and the present code; LLNL mechanism (bottom).***

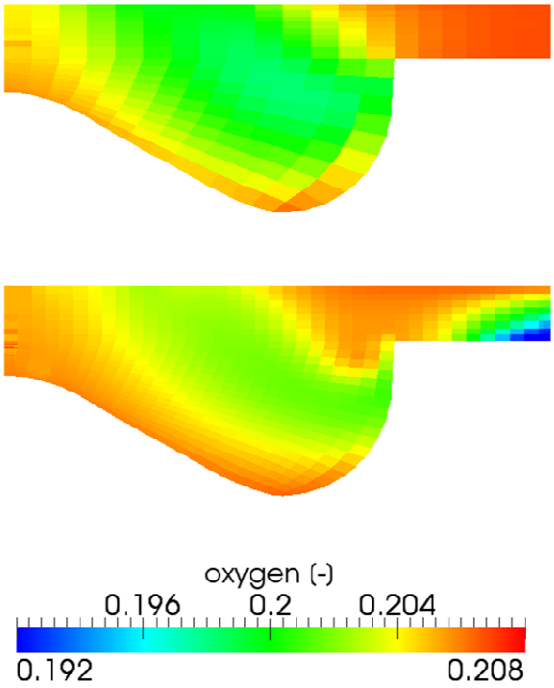


*Figure 8 – Oxygen mass fraction on vertical cut-plane at the injection axis, for the baseline case at -16° ATDC crank angle. Coarse (top) vs. refined (bottom) grid.*

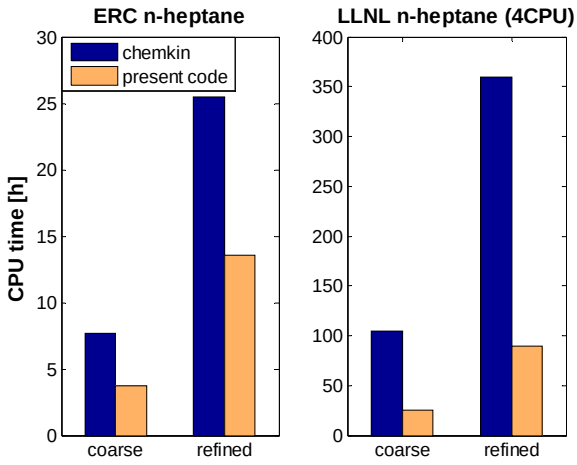


*Figure 9 – CPU times for the ERC n-heptane mechanism (left), LLNL n-heptane mechanism (right); KIVA-4 with Chemkin (blue) vs. present code (orange) coupling.*

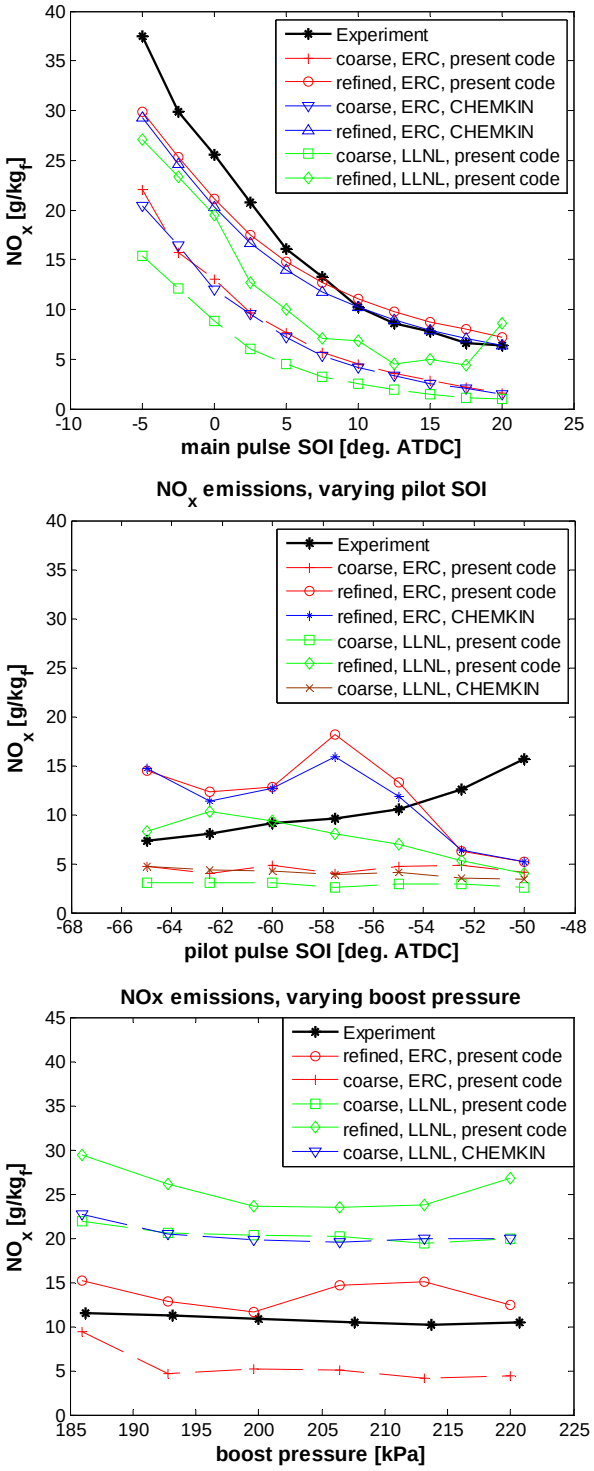


***Figure 10 – Predicted NOx emissions with varying main pulse start of injection (top), pilot pulse start of injection (center), intake boost pressure (bottom).***

As the same standard chemistry for NOx ($NO + NO_2$) was introduced into both reaction mechanisms, the predicted NOx emissions indicate how the local temperature distribution is predicted within the combustion chamber. From Figure 10, a fairly good match between the predicted and the experimental values is seen when varying the main injection pulse timing, especially when using the refined grid, where not only the trends but also the effective values have been caught by the simulations, especially for the late injection cases, where the main injection pulse has no interference with the heat release phase due to combustion of the pilot injection mixture.

The same trend with varying main SOI is predicted with the coarse mesh, but with lower values, with a fixed delta below the values predicted with the refined mesh. This happened also when using the LLNL mechanism, where even lower NOx values were predicted. Possibly, the lower spatial resolution – and consequently major temperature averaging due to bigger cell dimensions, may have lowered the predicted peak temperature values, leading to lower predicted NOx mass fractions. Similar differences in the predicted values between the coarse and refined grids were seen when sweeping the other parameters, i.e., the pilot pulse SOI and the intake boost pressure. The center and bottom plots of Figure 10 indeed show that the refined grid better catches the measured values. However, for these cases the averaging phenomenon of the coarse grid helps the simulation to reach the correct trends and perhaps mask or partially compensate for the grid-dependency of the spray models.

Finally, in all the simulations that were tested with both chemistry solvers, a very good consistency was noted, as was expected by the almost exact correspondence in the predicted species profiles observed when validating the code for a single cell, the adiabatic constant-volume reactor.

# CONCLUDING REMARKS

In the present paper the validation of a new code for the integration of reaction kinetics of gaseous mixtures has been presented and applied to modeling a heavy-duty, single-cylinder diesel engine, operating a two-stage combustion mode.

The code was developed to account for detailed reaction kinetics in practical internal combustion engine simulations, and exploits a sparse analytical Jacobian formulation that has been developed for arbitrary reaction mechanisms, and is presented in detail in [12]. The accuracy of the approach was first tested for adiabatic reactor cases, and with reaction mechanisms for diesel surrogates of very different sizes, ranging from few dozen species up to about one thousand species. Excellent agreement was found when comparing predicted species mass fraction profiles with the very well established CHEMKIN-II, reference chemistry code, and with significant computational time savings even for the smallest mechanism. The code was coupled to the KIVA-4 code and used to model a Caterpillar SCOTE 3401E engine for a variety of operating cases of Hardy [29]. The validation confirmed the accuracy of the overall approach, both in terms of the predicted in-cylinder pressure and heat release traces, and of nitrogen oxides, especially when considering a refined grid with a spatial resolution of about 1 millimeter.

As for the sparse analytical Jacobian chemistry code, and its suitability for practical combustion simulations in multidimensional domains, the main achievements can be summarized as follows:

- The overall speedups offered by the analytical Jacobian approach in comparison with the reference chemistry solver ranged from about 2 times for the smaller ERC mechanism up to more than 30 times for the large LLNL PRF mechanism. Thus, the code appears particularly suitable for semi-detailed or detailed reaction mechanisms to be incorporated into multidimensional combustion simulations, without needing to reduce the combustion mechanism size, while providing a fast solution even with small and dense mechanisms;

- The solver appeared to be robust even when used in multidimensional engine simulations, where the overall integration time is determined by the fluid flow solver, and where a variety of reacting conditions are simulated during the whole engine cycle;

- The computational capabilities of the approach were aided by the adoption of the LSODES ODE solver. The solver relies on sparse matrix algebra, where the Jacobian matrix can be introduced in sparse form. This points out the possibility to further improve the solver's capabilities by tailoring the ODE system integration method to the chemical kinetics problem.

- The overall CPU times required by the present KIVA-4 simulations when using the large LLNL n-heptane mechanism, and with parallel solution of the chemistry on 4 CPUs shows that the analytical Jacobian approach allows incorporation of

detailed chemistry while retaining reasonable computational times. The simulations ran in about 25 hours for the coarse grid, and about 4 days for the refined grid. Even further speedups may be achieved if the solution was run in parallel on multiple nodes, for instance using MPI, or on shared memory machines with multiple processors.

# REFERENCES


1. R. H. Stanglmaier, C. E. Roberts, "Homogeneous Charge Compression Ignition (HCCI): Benefits, Compromises, and Future Engine Applications", SAE technical paper 1999-01-3682, 1999.
2. S. L. Kokjohn, R. M. Hanson, D. A. Splitter, R. D. Reitz, "Fuel reactivity controlled compression ignition (RCCI): a pathway to controlled high-efficiency clean combustion", International Journal of Engine Research 12 (2011), 3:209-226.
3. S. C. Kong, R. D. Reitz, "Application of detailed chemistry and CFD for predicting direct injection HCCI engine combustion and emissions", Proceedings of the Combustion Institute 29 (2002), 1:663-669.
4. S. C. Kong, R. D. Reitz, "Use of Detailed Chemical Kinetics to Study HCCI Engine Combustion With Consideration of Turbulent Mixing Effects", Journal of Engineering for Gas Turbines and Power 124 (2002), 3:702-707.
5. W. J. Pitz, C. J. Mueller, "Recent progress in the development of diesel surrogate fuels", Progress in Energy and Combustion Science 37 (2011), 3:330-350.
6. Y. Ra, R. D. Reitz, "A combustion model for IC engine combustion simulations with multi-component fuels", Combustion and Flame 158 (2011), 1:69-90.
7. T. Lu, C. K. Law, "Toward accommodating realistic fuel chemistry in large-scale computations", Progress in Energy and Combustion Science 35 (2009), 2:192-215.
8. O. Herbinet, W. J. Pitz, C. K. Westbrook, "Detailed chemical kinetic mechanism for the oxidation of biodiesel fuels blend surrogate", Combustion and Flame 157 (2010), 5:893-908.
9. U. Maas, S. B. Pope, "Simplifying chemical kinetics: Intrinsic low-dimensional manifolds in composition space", Combustion and Flame 88 (1992), 34:239-264.
10. S. Lam, D. Coussis, "Understanding complex chemical kinetics with computational singular perturbation", Symposium (International) on Combustion 22 (1989), 931-941.
11. T. Lu, C. K. Law, "A directed relation graph method for mechanism reduction", Proceedings of the Combustion Institute 30 (2005), 1333-1341.
12. F. Perini, E. Galligani, R. D. Reitz, "An analytical Jacobian approach to sparse reaction kinetics for computationally efficient combustion modelling with large reaction mechanisms", Energy & Fuels (2012), DOI: 10.1021/ef300747n.
13. J. M. W. Chase, J. L. Curnutt, J. J. R. Downey, R. A. McDonald, A. N. Syverud, E. A. Valenzuela, "Janaf thermochemical tables", Journal of Physical and Chemical Reference Data 11 (1982) 3:695-940.
14. F. Perini, "Optimally reduced reaction mechanisms for Internal Combustion Engines running on biofuels", Ph. D. Thesis, University of Modena and Reggio Emilia, 2011. http://www.himech-phdschool.unimore.it/site/home/download/tesi-di-dottorato/documento92016812.html
15. R. J. Kee, F. M. Rupley, J. A. Miller, "CHEMKIN-II: A Fortran Chemical Kinetics package for the analysis of gas-phase chemical kinetics", Sandia Laboratories Report, SAND 89-8009B, 1989.
16. F. Perini, G. Cantore, R. D. Reitz, "An analysis on time scale separation for Internal Combustion Engine simulations with detailed chemistry", SAE technical paper 2011-24-0028, 2011.
17. D. A. Schwer, J. E. Tolsma, W. H. Green, P. Barton, "On upgrading the numerics in combustion chemistry codes", Combustion and Flame 128 (2002), 3:270-291.
18. A. F. Wagner, D. M. Wardlaw, "Study of the recombination reaction methyl + methyl => ethane. 2. Theory", The Journal of Physical Chemistry 92 (1988), 9:2462-2471.
19. A. Patel, S. Kong, R. Reitz, "Development and validation of a reduced reaction mechanism for HCCI engine simulations", SAE Technical Paper 2004-01-0558, 2004.
20. R. Seiser, H. Pitsch, K. Seshadri, W. Pitz, H. Curran, "Extinction and autoignition of n-heptane in counterflow configuration", Proceedings of the Combustion Institute 28 (2000) 2:2029-2037.
21. H. J. Curran, P. Gaffuri, W. J. Pitz, and C. K. Westbrook, "A Comprehensive Modeling Study of iso-Octane Oxidation", Combustion and Flame 129 (2002), 253-280.
22. O. Herbinet, W. J. Pitz, C. K. Westbrook, "Detailed chemical kinetic oxidation mechanism for a biodiesel surrogate", Combustion and Flame 154 (2008), 3:507-528.
23. F. Perini, J. L. Brakora, R. D. Reitz, G. Cantore, "Development of reduced and optimized reaction mechanisms based on genetic algorithms and element flux analysis", Combustion and Flame 159 (2012), 1:103-119.
24. P. N. Brown, G. D. Byrne, A. C. Hindmarsh, "VODE: A Variable-coefficient ODE solver", SIAM Journal on Scientific and Statistical Computing 10 (1989), 5:1038-1051.
25. A. Hindmarsh, "Odepack, a systematized collection of ODE solvers", IMACS Transactions on Scientific Computation 1 (1983), 55-64.

26. A. C. Hindmarsh, “LSODE and LSODI, two new initial value ordinary differential equation solvers”, ACM SIGNUM Newsletter 15 (4) (1980), 10-11.
27. G. D. Byrne, A. M. Dean, “The numerical solution of some kinetics models with VODE and CHEMKIN II”, Computers & Chemistry 17 (1993), 3:297-302.
28. D. J. Torres, M. F. Trujillo, “KIVA-4: An unstructured ALE code for compressible gas flow with sprays”, Journal of Computational Physics 219 (2006), 2:943-975.
29. W. L. Hardy, “An Experimental Investigation of Advanced Diesel Combustion Strategies for Emissions Reductions in a Heavy-Duty Diesel Engine at High Speed and Medium Load”, M. Sc. Thesis, University of Wisconsin-Madison, 2005.
30. B. A. Cantrell, H.-W. Ge, R. D. Reitz, C. J. Rutland, “Validation of Advanced Combustion Models Applied to Two-Stage Combustion in a Heavy Duty Diesel Engine”, SAE technical paper 2009-01-0714, 2009.
31. E. Musu, R. Rossi, R. Gentili, R. D. Reitz, “Heavy Duty HCPC”, SAE tecnical paper 2011-01-1824, 2011.
32. N. Abani, A. Munnannur, R. D. Reitz, “Reduction of Numerical Parameter Dependencies in Diesel Spray Models”, Journal of Engineering for Gas Turbines and Power 130 (2008), 3: 032809, 9 pages.
33. R. Reitz, F. Bracco, “On the dependence of spray angle and other spray parameters on nozzle design and operating conditions”, SAE Technical paper 790494, 1979.
34. F. Perini, E. Mattarelli, “Development and calibration of an enhanced quasi-dimensional combustion model for HSDI diesel engines”, International Journal of Engine Research 12 (2011), 311-335.
35. G. P. Smith, D. M. Golden, M. Frenklach, N. W. Moriarty, B. Eiteneer, M. Goldenberg, C. T. Bowman, R. K. Hanson, S. Song, W. C. Gardiner, Jr., V. V. Lissianski, Z. Qin, GRI-mech 3.0, http://www.me.berkeley.edu/gri_mech/.
36. B. Chapman, G. Jost, R. van der Pas, “Using OpenMP”, MIT Press, 2007. ISBN: 0-262-53302-2.

## CONTACT INFORMATION

Federico Perini
Dipartimento di Ingegneria Meccanica e Civile
Università di Modena e Reggio Emilia
strada Vignolese, 905/B – 41125 Modena, Italy
Ph.: +39 – 059 – 2056100
email: federico.perini@unimore.it

## ACKNOWLEDGMENTS

VM Motori (Cento, Italy) is gratefully acknowledged for supporting the present work with a research grant.